Biochimica et Biophysica Acta 1787 (2009) 609–616

Contents lists available at ScienceDirect

Biochimica et Biophysica Acta

journal homepage: www.elsevier.com/locate/bbabio

Role of phospholipids in respiratory cytochrome bc_1 complex catalysis and supercomplex formation ☆

Tina Wenz [a], Ruth Hielscher [b], Petra Hellwig [b], Hermann Schägger [c], Sebastian Richers [a], Carola Hunte [a,*]

[a] Max Planck Institute of Biophysics, Department of Molecular Membrane Biology, D-60438 Frankfurt, Germany
[b] Laboratoire de spectroscopie vibrationnelle et électrochimie des biomolécules, Institut de Chimie, UMR 7177, CNRS, Université de Strasbourg, 1 rue Blaise Pascal, F-67070 Strasbourg, France
[c] Zentrum der Biologischen Chemie, Cluster of Excellence "Macromolecular Complexes", Universitätsklinikum Frankfurt, 60590 Frankfurt, Germany

ARTICLE INFO

Article history:
Received 9 December 2008
Received in revised form 17 February 2009
Accepted 17 February 2009
Available online 28 February 2009

Keywords:
Mitochondria
Respiratory complex III
Cytochrome bc1 complex
Cardiolipin
Supercomplex

ABSTRACT

Specific protein–lipid interactions have been identified in X-ray structures of membrane proteins. The role of specifically bound lipid molecules in protein function remains elusive. In the current study, we investigated how phospholipids influence catalytic, spectral and electrochemical properties of the yeast respiratory cytochrome bc_1 complex and how disruption of a specific cardiolipin binding site in cytochrome c_1 alters respiratory supercomplex formation in mitochondrial membranes. Purified yeast cytochrome bc_1 complex was treated with phospholipase A_2. The lipid-depleted enzyme was stable but nearly catalytically inactive. The absorption maxima of the reduced *b*-hemes were blue-shifted. The midpoint potentials of the *b*-hemes of the delipidated complex were shifted from −52 to −82 mV (heme b_L) and from +113 to −2 mV (heme b_H). These alterations could be reversed by reconstitution of the delipidated enzyme with a mixture of asolectin and cardiolipin, whereas addition of the single components could not reverse the alterations. We further analyzed the role of a specific cardiolipin binding site (CL_i) in supercomplex formation by site-directed mutagenesis and BN-PAGE. The results suggested that cardiolipin stabilizes respiratory supercomplex formation by neutralizing the charges of lysine residues in the vicinity of the presumed interaction domain between cytochrome bc_1 complex and cytochrome *c* oxidase. Overall, the study supports the idea, that enzyme-bound phospholipids can play an important role in the regulation of protein function and protein–protein interaction.

1. Introduction

Lipids are essential components of every cell. Lipid bilayers form boundaries to separate different cell compartments and they provide the matrix for membrane-spanning proteins. A vast number of studies suggest that specific association of lipids with membrane proteins can contribute to functional aspects of the protein [1] affecting, for instance, enzyme activity [2], channel function [3] and drug action [4]. Only recently has it been possible to obtain crystal structures of membrane proteins with sufficient resolution to identify bound lipids. It is now recognized that retained or supplemented lipids are important for integrity and successful crystallization of membrane proteins (for recent review see [5]). Characteristic binding motifs for the phosphodiester of lipid head groups and a specific cardiolipin (CL, bisphosphatidyl glycerol) binding motif have been deduced from available membrane protein structures [6,7]. Identification of specific lipid-binding sites enables analysis by site-directed mutagenesis to understand the role of bound phospholipids. For example, altering the primary ligand of the interhelical phosphatidyl-inositol in the yeast cytochrome bc_1 complex (cyt bc_1 complex) destabilizes the interaction of the Rieske protein subunit with the catalytic core of the enzyme [8]. Mutational analysis of a conserved lipid-binding site in subunit III of the cytochrome *c* oxidase (COX) from *Rhodobacter sphaeroides* identified by X-ray crystallography [9] points to a crucial role of the bound lipid in the interaction of subunit I and III [10].

The role of specific protein–lipid interactions have been studied in the mitochondrial cyt bc_1 complex (ubiquinol:cytochrome *c* oxidoreductase, EC 1.10.2.2, complex III). The multi-subunit protein complex embedded in the inner mitochondrial membrane catalyzes the transfer of electrons from membrane-localized ubiquinol to water-soluble cytochrome *c* (cyt *c*). This redox reaction is coupled to translocation of protons across the membrane. The mechanism that links proton translocation to electron transfer, the protonmotive Q

Abbreviations: Cyt, cytochrome; CL, cardiolipin; COX, cytochrome *c* oxidase; BN-PAGE, blue native polyacrylamide gel electrophoresis; UM, undecyl-maltopyranoside

☆ This work was supported by the Deutsche Forschungsgemeinschaft, Sonderforschungsbereich 472, Projects P11 (H.S.), P17 (C.H.), P24 (P.H.) and by the Cluster of Excellence "Macromolecular Complexes" at the Goethe University Frankfurt (DFG Project EXC 115 C.H, H.S.).

* Corresponding author. Present address: Institute of Membrane and Systems Biology, University of Leeds, Leeds LS2 9JT, UK. Tel.: +44 113 3437750; fax: +44 113 3434228.
E-mail address: c.hunte@leeds.ac.uk (C. Hunte).

0005-2728/$ – see front matter © 2009 Elsevier B.V. All rights reserved.
doi:10.1016/j.bbabio.2009.02.012

cycle [11], depends on two spatially separated binding sites for ubiquinol and ubiquinone, both located in the cytochrome *b* (cyt *b*) subunit. The key step of the mechanism is the bifurcated route of the two electrons released upon ubiquinol oxidation at the Q_o site. One electron is transferred into the high potential chain, the 2Fe–2S cluster Rieske protein (ISP) and cytochrome c_1 (cyt c_1), and subsequently delivered to cyt *c*. The second electron is transferred via the low potential chain, heme b_L and heme b_H of cyt *b* to the Q_i site, where quinone is reduced to semiquinone. For a complete turnover of the enzyme, a second ubiquinol molecule is oxidized in the same way so that the Q_i-site semiquinone is reduced and an ubiquinol leaves this pocket. X-ray structures from the bovine [12,13], avian [14] and yeast [15–17] complexes provided critical information for elucidation of mechanism and structure/function relationships [5,18–20].

Phospholipids are essential for the function of the cyt bc_1 complex. Delipidation of the bovine complex leads to reversible loss of catalytic activity [21,22]. Restoration of activity depends on CL leading to the postulate that "CL is either essential for catalytic function, or that it acts as an allosteric ligand that stabilizes the fully active conformation" [23]. Several tightly bound phospholipids including CL were identified in X-ray structures of the yeast cyt bc_1 complex [7,8,24] (Fig. 1A, B). Less detergent in solubilisation and chromatography steps increased the number of structurally resolved endogenous lipids [17]. Destabilization of individual phospholipid-binding sites in the yeast cyt bc_1 complex by site-directed mutagenesis, suggested that these phospholipids are important for the structural and functional integrity of the membrane protein [8]. One CL molecule is found in a depression formed by cyt *b*, cyt c_1, and ISP close to the site of ubiquinone reduction, the Q_i site. It is mainly stabilised by residues K288, K289 and K296 of subunit cyt c_1. This CL molecule, henceforth addressed as CL_i (see Fig. 1B) appears to stabilize the architecture of the proton conducting environment at the Q_i site and may be involved in proton uptake [8,25]. Phospholipids and especially CL, which is in non-photosynthetic eukaryotes exclusively found in the inner mitochondrial membrane, are also important for the supramolecular association of the cyt bc_1 complex with COX. In yeast, CL deficiency causes destabilization of supercomplexes [26].

In the present work, we investigate in detail the effects of enzymatic delipidation of the yeast cyt bc_1 complex on its catalytic, spectral and electrochemical properties. We further analyzed, if alterations in the delipidated enzyme can be reversed by addition of phospholipids. Additionally, the role of the specific CL_i-binding site of yeast cyt bc_1 complex for the formation of respiratory supercomplexes was examined by site-directed mutagenesis and BN-PAGE analysis.

2. Materials and methods

2.1. Media and yeast strains

Premixed media were from ForMedium. Yeast strains were grown in YPG (1% yeast extract, 2% peptone and 3% glycerol) and/or in media containing 3% lactate in 5 l baffled flasks (2 l culture volume) at 30 °C and 220 rpm to OD_{550} of 8–10. Generation of expression plasmids for lysine substitutions of the cyt c_1 subunit of the cyt bc_1 complex has previously been described [8]. The plasmids containing wild-type and mutated *CYT1* genes were transformed into the yeast strain LLD6, in which the *CYT1* gene is deleted [8]. Additionally, the plasmids were also transformed into a yeast strain, in which both the *CYT1* and the *CRD1* (cardiolipin synthase) genes are deleted. This strain was constructed by targeted substitution of the *CRD1* gene in LLD6 by a kanMX4 cassette using the plasmid pYORC_YDL142c, which was obtained from Euroscarf. The strains used in this study are listed in Table 1.

2.2. Phospholipids

Asolectin from soybean and cardiolipin from bovine heart were obtained from Sigma. Asolectin contains roughly equal proportions of lecithin, cephalin and phosphatidyl-inositol with minor amounts of other phospholipids and polar lipids.

2.3. Purification of cytochrome bc_1 complex

The wild-type yeast strain was grown in YPG medium. Mitochondrial membranes were prepared as described [27]. Cyt

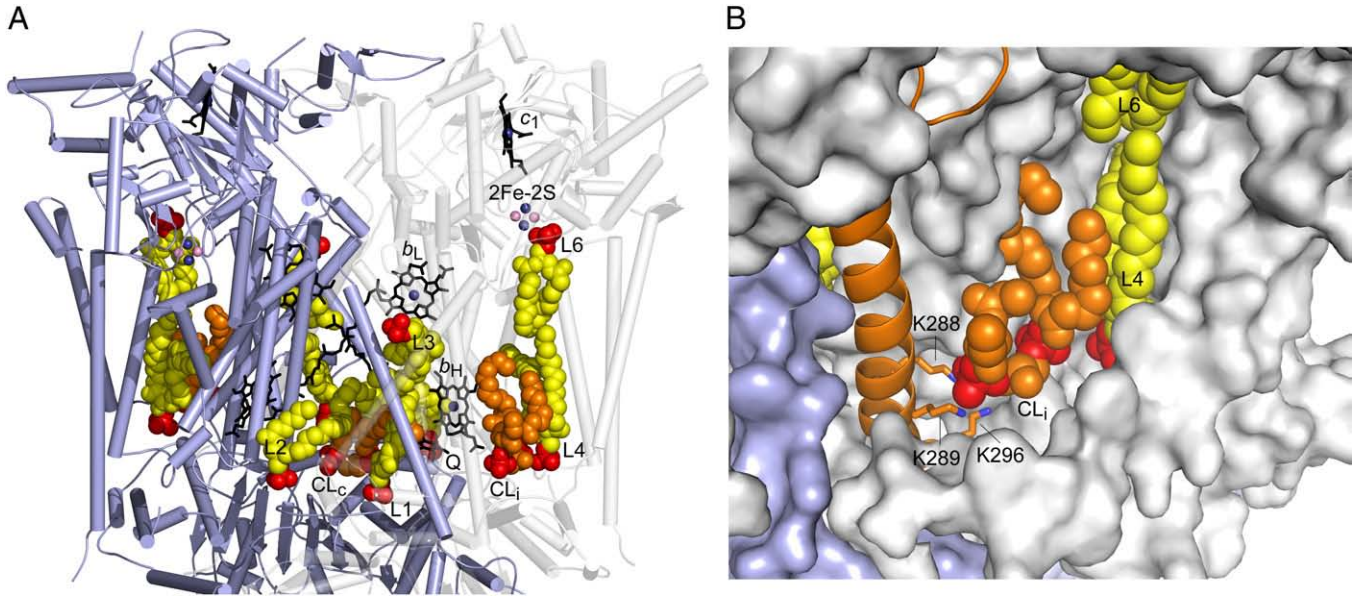

Fig. 1. Yeast cyt bc_1 complex with bound lipids (PDB entries 1P84, 3CX5). (A) Overview of the dimeric structure with one functional monomer in blue and the other in transparent grey. Lipids are presented as sphere models in yellow and cardiolipin (CL) is highlighted in orange. All atoms of phosphate groups are shown in red. With the exception of CL all phospholipids are labelled according to [7] and their head groups are truncated to phosphate for clarity. L4 and L6 reflect the position of the membrane bilayer. The Q_i site with ubiquinone (Q) and heme b_H is surrounded by lipids including the surface exposed CL_i and the central CL_c [24]. The latter was resolved at the centre of the monomer interface in the high-resolution structure. (B) Detailed view of the CL_i-binding site close to the Q_i site. Subunit cyt c_1 is shown as orange cartoon representation and its residues K288, K289 and K296 interacting with CL_i are shown as stick models in orange with blue nitrogen atom. Residual protein subunits are presented as surface model and colors are as described above.

Table 1
Yeast strains used for the analysis of CL_i-dependent supercomplex formation.

Name	Genotype	Reference
LLD6 (= Δcytc1)	Mat a, Ade2–1, his3–11 and 3–15, trp 1–1, leu 2–3 and 2–112, ura 3–1, can 1–100, cytc1::His	[38]
wt	LLD6 [wt Cytc1]	[8]
K288L	LLD6 [K228L Cytc1]	[8]
K289L	LLD6 [K289L Cytc1]	[8]
K296L	LLD6 [K296L Cytc1]	[8]
K288L/K289L	LLD6 [K288L/K289L Cytc1]	[8]
K288L/K296L	LLD6 [K288L/K296L Cytc1]	[8]
K289L/K296L	LLD6 [K289L/K296L Cytc1]	[8]
K288L/K289L/K296L	LLD6 [K288L/K289L/K296L Cytc1]	[8]
Δcrd	LLD6 crd1::kanMX4 [wt Cytc1]	This study
Δcrd/K228L	Δcrd [K228L Cytc1]	This study
Δcrd/K289L	Δcrd [K289L Cytc1]	This study
Δcrd/K296L	Δcrd [K296L Cytc1]	This study
Δcrd/K288L/K289L	Δcrd [K288L/K289L Cytc1]	This study
Δcrd/K288L/K296L	Δcrd [K288L/K296L Cytc1]	This study
Δcrd/K289L/K296L	Δcrd [K289L/K296L Cytc1]	This study
Δcrd/K288L/K289L/K296L	Δcrd [K288L/K289L/K296L Cytc1]	This study

Single, double and triple leucine replacements of the cyt c_1 residues K288, K289 and K296, the primary stabilizing ligands of CL_i, were analyzed in a CL-wild type (LLD6) and a CL-deficient strain (Δcrd1).

bc_1 complex was purified using two consecutive DEAE anion exchange chromatography steps as described previously [27]. Membranes were solubilized at a protein concentration of 10 mg/ml with 1.5% dodecyl-maltopyranoside. The detergent was exchanged to 0.05% (w/v) undecyl-maltopyranoside (UM) at the second DEAE step.

2.4. Redox spectroscopy and quantification of cytochrome bc_1 complex

Wild-type, delipidated and relipidated complexes were diluted to ~10 μM in assay buffer (see below). Redox difference spectra were quantified using extinction coefficients of 17.5 mM^{-1} cm^{-1} for ascorbate-reduced minus ferricyanide-oxidized *c*-heme (553–540 nm) and 25.6 mM^{-1} cm^{-1} for dithionite-reduced minus ferricyanide-oxidized *b*-hemes (562–575 nm).

2.5. Delipidation and relipidation

Purified cyt bc_1 complex was diluted to 15 μM in 2 mM $CaCl_2$, 50 mM Tris–HCl pH 7.4, 250 mM NaCl, 0.05% UM. The enzyme was delipidated by incubation with 66 U/ml phospholipase A_2 (porcine pancreatic, Sigma) for 1 h at room temperature. Delipidation was stopped by addition of 10 mM EDTA. For relipidation, asolectin or cardiolipin or a mixture of both lipids was added from 2% (w/v) sonified lipid/water suspensions to 15 μM cyt bc_1 complex at a final concentration of 132 μM and 69 μM for asolectin and cardiolipin, respectively, and incubated for 1 h at RT. The enzyme/lipid mixture was used immediately or stored at 4 °C for a maximum of 3 days.

2.6. Measurement of ubiquinol–cytochrome c reductase activity

Purified cyt bc_1 complex was assayed in 50 mM potassium phosphate pH 7.4, 250 mM sucrose, 1 mM KCN, 0.05% UM, and 50 μM horse heart cyt *c* at room temperature for ubiquinol-dependent cyt *c* reductase activity. The enzyme was diluted to 2.5–10 nM in assay buffer and the reaction was started with 40 μM decylubiquinol. Reduction of cyt *c* was monitored at 550 nm versus 540 nm in dual wavelength mode and the rate of cyt *c* reduction was calculated using an extinction coefficient of 21.5 mM^{-1} cm^{-1}. Turnover numbers are expressed as mol cyt *c* reduced per mol cyt bc_1 complex monomer per second under steady-state condition.

2.7. Spectroelectrochemistry

An ultrathin layer spectroelectrochemical cell for the UV/Vis range was used as previously described [28]. Cyt bc_1 complex samples with different lipid content were used at a concentration of ~70 mg/ml in 50 mM Tris pH 7.3, 250 mM NaCl, 0.05% UM. The gold grid working electrode was chemically modified with a 1:1 mixture of 2 mM cysteamine and 2 mM mercaptopropionic acid solution and 16 different mediators were added to a final concentration of 45 μM each to accelerate the redox reaction as reported previously [29]. Potentials were measured with an Ag/AgCl/3M KCl reference electrode and are quoted in reference to the standard hydrogen electrode at pH 7.0.

The redox dependent signal of each heme could be differentiated in electrochemically induced UV/Vis difference spectra, on the basis of the relative contribution of the hemes b_L, b_H and c_1 to each position in the alpha band. The contributions were obtained on the basis of redox titrations that were performed by stepwise setting of potentials and recording the spectrum after equilibration. Typically, data were recorded using 50 mV steps between −0.29 V and 0.71 V. All measurements were performed at 5 °C. The pH was adjusted in 50 mM Tris buffer (pH 7.3). The reference electrode was calibrated with the cyclovoltammogram of a buffered $K_4[Fe(CN)_6]$ solution before the potential titration was started. All electrochemical titrations were reversible as controlled by directly comparing fully oxidized minus fully reduced visible difference spectra at different points in the experiments. Data analysis was carried out with a program developed by S. Grzybek termed E_HTIT [30], in which the midpoint potentials E_m and the number *n* of the transferred electrons were obtained by adjusting a calculated Nernst curve to the measured absorbance change at a chosen single wavelength (563 nm, where all three hemes contribute), using the best fit for data evaluation. This analysis was confirmed for several wavelengths. Typically, an *n* value of about 0.9 was found for each heme. Electrochemically induced difference spectra were recorded and processed as previously described [29].

2.8. Analysis of respiratory supercomplex formation in yeast mitochondria by blue native electrophoresis

Yeast strains listed in Table 1 were grown with lactate as a carbon source. Mitochondria were then isolated as described [31] and stored at −80 °C as 400 μg aliquots. Mitochondrial pellets were solubilized for BN-PAGE using a digitonin/protein ratio of 3 g/g as described previously [32]. Equal protein amounts based on Lowry assay were loaded on all gels. Following BN-PAGE, 0.5 cm strips from BN-PAGE were excised and analyzed in a second dimension by Tricine-SDS-PAGE [33].

3. Results

3.1. Delipidation of yeast cytochrome bc_1 complex

Detergent solubilised and purified yeast cyt bc_1 complex contains at least six tightly bound phospholipid molecules per enzyme monomer as resolved in X-ray structures of the complex [7,8,24]. Residual electron density in these structures suggests the presence of additional less ordered lipids. Phospholipase A_2 cleaves the acyl bond at the sn-2 position in phospholipids generating lyso-phospholipids and fatty acids. Treatment of the bovine cyt bc_1 complex with this enzyme resulted in a lipid-depleted and inactive protein [23]. Following this protocol, purified yeast cyt bc_1 complex was incubated with phospholipase A_2 to remove enzyme-bound phospholipids. The extent of delipidation was followed by monitoring the decrease of cyt *c* reductase activity in 10 min intervals. After 1 h incubation, the turnover number has decreased to about 10% of the original value

(Fig. 2). Longer incubation with phospholipase did not result in a further decrease. Incubation of the native enzyme with EDTA-inactivated phospholipase did not alter the catalytic activity.

Delipidated bovine cyt bc_1 complex can be repurified by anion exchange chromatography without apparent destabilization of the multi-subunit complex [23]. In contrast, repurification attempts of the delipidated yeast complex resulted in aggregation of the protein. Yet, the phospholipase-delipidated complex was stable for one week at 4 °C and in this time frame no aggregation of the protein or loss of subunits was observed as judged by SDS-PAGE and Western blot analysis (data not shown). Therefore, the delipidated complex was not further purified and used in mixture with the EDTA-inactivated phospholipase for further analysis.

3.2. Effects of delipidation and relipidation on cytochrome c reductase activity

The delipidated, nearly inactive but stable yeast cyt bc_1 complex was incubated for 1 h with asolectin or cardiolipin or a mixture of both. The final concentrations were 15 μM complex and 0.01% total lipid. Addition of asolectin resulted only in a minor increase of the enzyme activity (Fig. 2). Increasing amounts of asolectin or prolonged incubation did not further enhance the turnover number (data not shown). Upon addition of cardiolipin to the delipidated complex, the enzyme activity increased to about 20% of the wild-type complex (Fig. 2). As with the asolectin treatment, increasing amounts of CL or a longer incubation time did not lead to further reactivation. Addition of a high excess of phospholipids to the delipidated complex resulted in precipitation of the enzyme. Maximum reactivation of the delipidated enzyme was observed after addition of a mixture of asolectin and cardiolipin. About 70% of the original turnover number could be restored (Fig. 2). Addition of asolectin, CL or the asolectin/CL mixture to the untreated enzyme did not alter its activity.

3.3. Effects of delipidation and relipidation with different phospholipids on the redox-spectroscopical characteristics of the cytochrome bc_1 complex

Redox spectra of the untreated, delipidated and relipidated complex were recorded to analyze perturbations of the heme cofactors upon delipidation. The delipidation caused a blue shift of the *b*-heme absorption maximum from 563 nm in the untreated wild-type enzyme to 561 nm in the delipidated enzyme (Fig. 3). Delipidation-related changes in the *c*-heme absorption maximum were not resolved. Addition of asolectin to the delipidated enzyme did not change the position of the *b*-heme maximum at 561 nm. However, relipidation with cardiolipin caused a slight shift of the *b*-heme maximum to 562 nm. Upon addition of a mixture of asolectin and cardiolipin, the position of the *b*-heme maximum was nearly identical to the untreated enzyme demonstrating reversibility of the blue shift (Fig. 3). Addition of asolectin, CL or the asolectin/CL mixture to the untreated enzyme did not alter the position of the *b*-heme alpha-band maximum (data not shown).

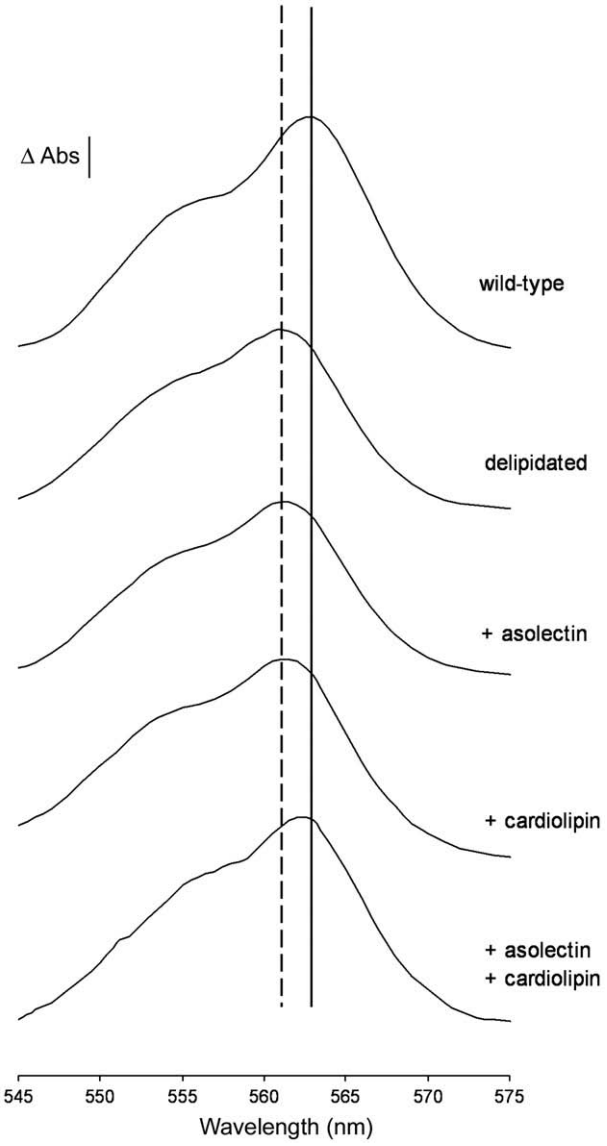

Fig. 3. Spectral properties of wild-type, delipidated and relipidated yeast cyt bc_1 complex. Difference spectra were recorded for sodium dithionite-reduced vs ferricyanide-oxidized cyt bc_1 complex. The solid line indicates the alpha-band maximum of cyt *b* in the wild-type enzyme, the dashed line in the phospholipase-treated enzyme.

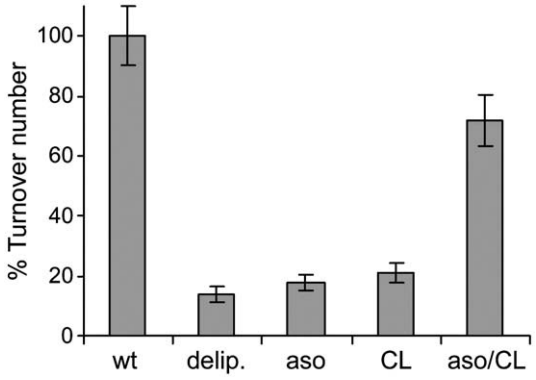

Fig. 2. Cyt *c* reductase activity from wild-type, delipidated and relipidated yeast cyt bc_1 complex. Relative turnover numbers are shown for the wild-type enzyme (wt), delipidated enzyme (delip), relipidated enzyme with asolectin (aso), CL (CL), or a mixture of asolectin and CL (aso/CL) added. The rate of the wild-type cyt bc_1 complex is referred to as 100% value. The assay was carried out according to the standard protocol with 10 nM cyt bc_1 complex, 50 μM cyt *c* and 40 μM decylubiquinol. The values are the average of five measurements.

3.4. Effects of delipidation and relipidation with different phospholipids on the midpoint redox potentials of the b-hemes

For further characterization of the lipid-cofactor interplay, the midpoint redox potentials of the heme groups were determined as described in Material and methods for untreated, delipidated and relipidated cyt bc_1 complex. Fig. 4 shows the redox titration curves of the native untreated complex (A) in direct comparison to the lipid-depleted complex (B) and after supplementation of the complex with

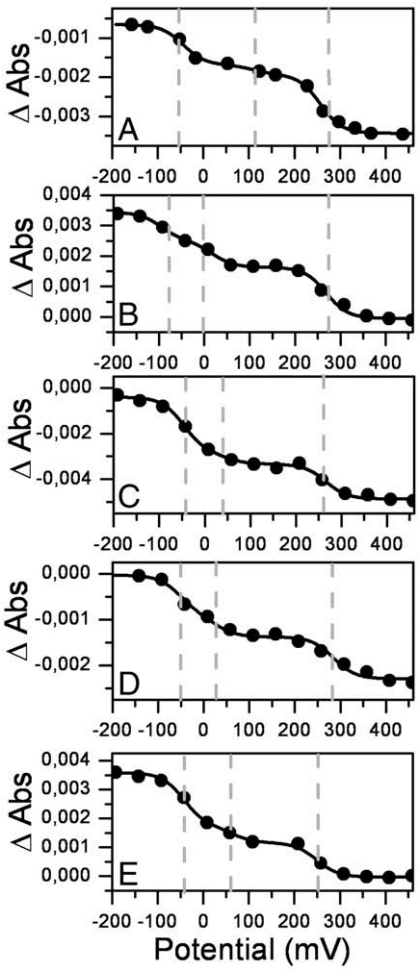

Fig. 4. Potential titrations of cyt bc_1 complex samples as isolated (A), delipidated (B), relipidated with asolectin and CL (C), relipidated with asolectin (D), and with CL (E) only. Oxidative and reductive titrations were fully reversible. For details see Materials and methods and Table 2.

a mixture of asolectin and CL (C) as well as addition of asolectin (D) and cardiolipin (E) alone. The midpoint potential of heme b_H of the untreated enzyme was 113 mV, whereas it was strongly shifted to the negative ($E_m = -2$ mV) in the lipid-depleted complex. This shift could be partially reversed (to $E_m = 26$ mV) by addition of asolectin to the delipidated enzyme. Addition of cardiolipin further raised the midpoint potential to 64 mV. Relipidation with the mixture of asolectin and CL raised the midpoint potential for heme b_H to 48 mV (Table 2).

The E_m of heme b_L was −52 mV for the untreated enzyme. A slight shift to a more negative value of −82 mV was determined for the lipid-depleted cyt bc_1 complex. In the asolectin treated enzyme, the midpoint potential was −51 mV. Addition of CL to the delipidated enzyme gave rise to a midpoint potential of −42 mV, similar to the effect of the asolectin/CL mixture (−46 mV).

An E_m of 278 mV was determined for heme c_1 of the untreated enzyme. No major changes were observed after lipid depletion or relipidation with asolectin, CL or a mixture of asolectin and CL. The midpoint potentials are summarized in Table 2.

3.5. Role of CL_i for supercomplex formation and stability

CL does not only influence the catalytic activity of the cyt bc_1 complex and the environment of the cofactors, but it has also been shown to be important to stabilize the supramolecular interaction between cyt bc_1 complex and COX. The CL_i molecule specifically bound close the Q_i site of the cyt bc_1 complex was suggested to be involved in linking the two complexes together [26]. Residues K288, K289 and K296 of subunit cyt c_1 are the primary ligands of CL_i (Fig. 1B). Their side chains interact with one phosphodiester group. To investigate the role of this specific CL, one, two or all three lysines had been substituted by leucine [8]. While the single mutations did not have a measurable effect on the ubiquinol:cyt *c* reductase activity, double and triple replacements resulted in a slow growth phenotype on non-fermentable carbon sources correlated with a lower cyt bc_1 complex content in mitochondrial membranes. All single, double and triple replacement mutants were now re-analysed with respect to supercomplex stabilization in mitochondrial membranes. Loss of positively charged lysine(s) was expected to reduce the affinity for the negatively charged CL, eventually leading to loss of CL_i-binding and potentially to destabilization of the cyt bc_1 complex:COX supercomplex. In addition, another set of yeast strains was constructed, which carried the same replacement variants but in a CL-free background. This was achieved by a knockout of the cardiolipin synthase (*CRD1*) in the nuclear genomic DNA. All analyzed variants are listed in Table 1.

Mitochondrial membrane preparations of each variant grown on lactate were analyzed by BN-PAGE and 2-D BN/SDS-PAGE. The wild-type (WT) (Fig. 5A, upper panel) and selected CL-containing variants containing one (K289L), two (K288L/K289L) and three (K288L/K289L/K296L) replacements (Fig. 5B–D, upper panels) were compared with the corresponding variants in a CL-free background (Fig. 5A–D, lower panels). For WT yeast (Fig. 5A, upper panel), larger supercomplex (L) comprising dimeric cyt bc_1 complex and two copies of COX was the predominant respiratory supercomplex. Yeast respiratory supercomplexes have been previously characterized [26,34] so that the type of supercomplex can be deduced from its position relative to the monomeric and dimeric ATP synthase and the detection of some cyt bc_1 complex and/or COX subunits. Smaller supercomplex (S) was hardly detectable. All CL-containing lysine variants (Fig. 5B–D, upper panels) also contained respiratory supercomplexes but there was a clear shift to the smaller supercomplex. For the triple replacement variant, also individual complexes cyt bc_1 complex and COX (red and green arrows, respectively, in Fig. 5D, upper panel) were observed after BN-PAGE. The results are consistent for the other single and double replacements (data not shown). These findings indicate that CL at the specific CL_i-binding site, which is most likely not occupied in triple (and double) replacement variants, contributes considerably to the stability of supercomplexes but is not essential for their formation.

A supercomplex stabilizing role for CL_i is suggested by the analysis of CL-free variants. In the CL-free environment, no stable supercomplex formation could be observed with the wild-type complex (Fig. 5A, lower panel) as shown before [26]. Introducing one single lysine replacement, i.e. the loss of one positive charge, could not restore supercomplex stability, as exemplified with the K289L variant in Fig. 5B, lower panel. Results for the K288L and K296L single replacement variants were highly similar (not shown). However, supercomplex stability was found to be restored in two double replacement variants, namely in the K288L/K289L variant, as shown in Fig. 5C, lower panel, and in the K289L/K296L variant (not shown)

Table 2
Midpoint redox potentials (mV) for wild-type (WT), delipidated and relipidated yeast cyt bc_1 complex vs. standard hydrogen electrode at pH 7.0.

	Heme b_L	Heme b_H	Heme c_1
WT	−52	113	278
delipidated	−82	−2	278
+ asolectin	−51	26	285
+ cardiolipin	−42	64	250
+ asolectin/cardiolipin	−46	48	266

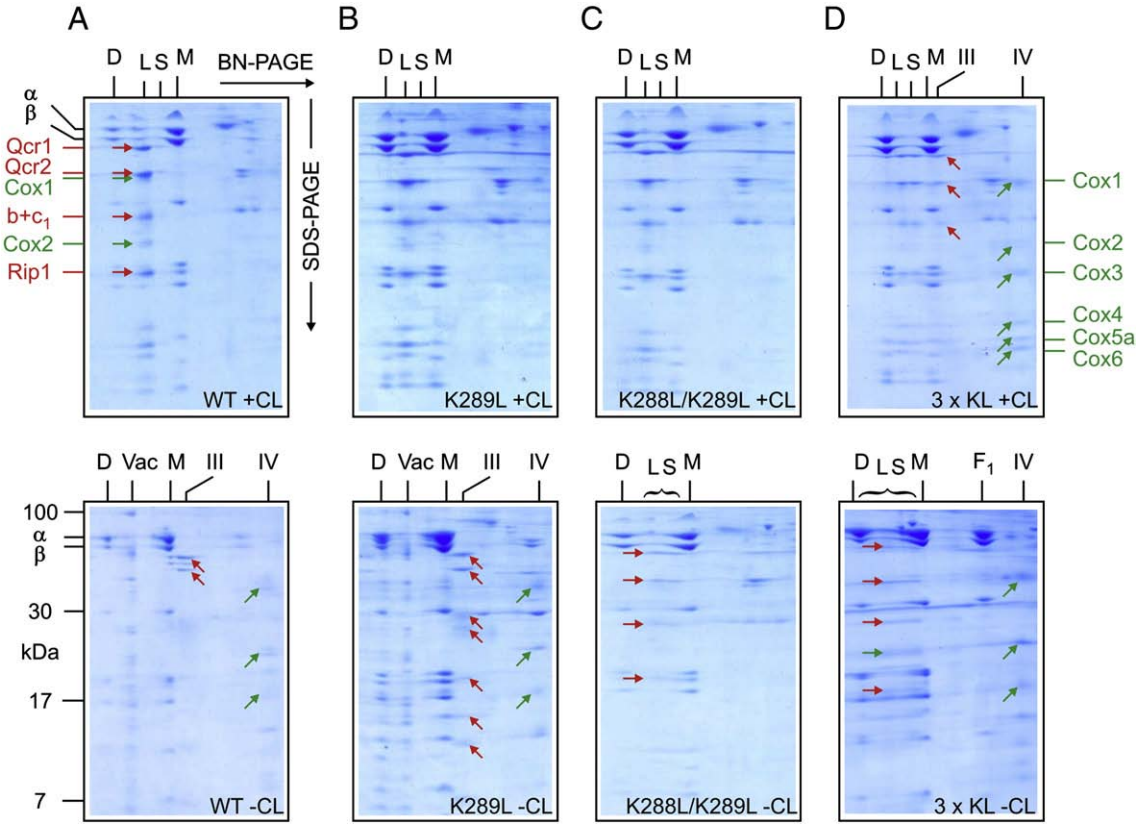

Fig. 5. Analysis of respiratory supercomplexes with mutations in the specific CL_i-binding site of cyt c_1 from CL-containing (upper panels) and CL-deficient yeast mitochondria (lower panels). Mitochondrial complexes from parental and mutant strains grown on lactate were solubilized with digitonin and separated by BN-PAGE. The subunits were then resolved by SDS-PAGE in the second dimension. Some characteristic subunits of cyt bc_1 complex (labelled QCR) and COX are indicated in red and green, respectively. The α and β subunits of ATP synthase are marked black. Horizontal and diagonal red and green arrows point to subunits of cyt bc_1 complex and COX in respiratory supercomplexes and individual complexes, respectively. M, D, monomeric and dimeric ATP synthase; L, S, larger and smaller respiratory supercomplexes; III, IV, individual cyt bc_1 complex and COX, respectively; Vac, vacuolar ATPase; F_1, F_1-part of ATP synthase. (A) Mitochondria from a CL-synthesizing (WT +CL) and a CL-deficient (WT −CL) parental strain were used. (B) Analysis of the K289L variant of cyt c_1 from CL-synthesizing (K289L +CL) and CL-deficient (K289L −CL) strains. (C) Analysis of the K288L/K289L double replacement in cyt c_1 from CL-synthesizing (K288L/K289L +CL) and CL-deficient (K288L/K289L −CL) strains. (D) Analysis of the K288L/K289L/K296L triple replacement in cyt c_1 from CL-synthesizing (3×KL +CL) and CL-deficient (3×KL −CL) strains.

but not in the K288L/K296L variant (not shown). Supercomplexes were identified also for the triple replacement variant, although the detection of free COX (green arrows in Fig. 5D, lower panel) pointed to reduced stability of supercomplexes.

4. Discussion

Information obtained from high-resolution X-ray structures of membrane proteins in recent years has highlighted an intimate relationship between these proteins and membrane lipids. Structurally resolved lipids with tight and specific binding sites appear to be important for structural and functional integrity of membrane proteins, yet the role of individual lipids and the underlying mechanism remain elusive so far. In this work, we investigated the effect of bound phospholipids on the function and biophysical properties of the yeast cyt bc_1 complex and on its supramolecular assembly with COX in mitochondrial membranes.

Enzymatic delipidation of the yeast cyt bc_1 complex was used to analyze effects on the catalytic activity of the complex and on the properties of cofactors. Previous research showed that the bovine cyt bc_1 complex can be inactivated by delipidation, either by phospholipase A_2 treatment or by a chromatography method [21]. Reactivation of the lipid-depleted bovine complex depended on addition of lipids, in particular of phosphatidyl-ethanolamine and phosphatidyl-choline. CL, which was not activating when added as single lipid, was needed to stabilize the native structure of the complex [23,21]. Similarly, delipidation nearly abolishes cyt *c* reductase activity of the yeast cyt bc_1 complex. The finding that the delipidated yeast complex could only be fractionally activated by addition of CL alone is in full agreement with previous reports on the reactivation of the bovine complex [21]. For the yeast complex, maximum reactivation (~70% of the initial value) was achieved by addition of a mixture of asolectin and CL.

Surprisingly, the spectral and electrochemical properties of the heme *b* cofactors were dependent on the lipid content of the enzyme. In the redox spectra of the delipidated enzyme, a blue shift of the alpha-band maximum of cyt *b* of about 2 nm was observed. This shift proved to be reversible and lipid-dependent. Addition of the asolectin/CL mixture, which provided maximum reactivation of the delipidated complex, resulted in peak positions of the *b*-hemes that were identical with the native enzyme. A small blue shift of 1.5–1.7 nm was also reported for the delipidated bovine complex, but only if the enzyme was repurified by chromatography [23]. Reversibility of that shift was not shown and no changes in the spectral properties of the delipidated bovine complex before repurification were reported.

In addition to the lipid-dependent position of the *b*-heme absorption maximum, the midpoint redox potentials of both *b*-hemes, b_H and b_L, were also influenced by enzyme-bound lipids. The E_m of heme b_L was shifted from −52 mV in the untreated complex to −82 mV in the delipidated complex. Heme b_L transfers electrons released upon ubiquinol oxidation at the Q_o site to heme b_H. The shift in the midpoint potential of heme b_L affects the electron transfer in the low potential chain. Addition of CL alone could only partly reverse this shift (−42 mV). After addition of the asolectin/CL mixture, the

midpoint potential of heme b_L was comparable to the native enzyme. This finding is in accordance with the analysis of the catalytic activity and the peak position of the *b*-hemes in the redox spectra upon delipidation and relipidation. Addition of asolectin or CL alone led only to a minor increase of the turnover number, whereas a ~70% recovery was detected for the relipidation with the asolectin/CL mixture. This phospholipid mixture could also completely reverse the blue shift of the *b*-heme peak position in the redox spectra in contrast to addition of asolectin and CL alone.

The effect of delipidation for heme b_H was even more pronounced than for heme b_L as its E_m shifted from 113 mV to −2 mV. This shift is partially reversible when adding back CL or the asolectin/CL mixture, though to a considerable lesser extent than in the case of heme b_L. Heme b_H reduces quinone or the semiquinone radical at the Q_i site according to the Q cycle. The shift of the midpoint potential to more negative values and the difference in the midpoint potential of heme b_H and b_L, which is changed significantly from the native (165 mV) to the delipidated enzyme (80 mV), will decrease the driving force for and the extent of electron transfer through the *b*-hemes to the Q_i site. This creates a disbalance between high and low potential chain which could provoke generation of reactive oxygen species at the Q_o site [27,35,36]. How does the removal of lipids affect the midpoint potential of the heme groups? One can safely assume that the lipid-binding sites resolved in the crystal structures of the yeast cyt bc_1 complex are also occupied in the purified complex as confirmed by analysis of extracted lipids from both samples (Richers and Hunte, in prep). Clearly, more lipids are tightly bound in the vicinity of the Q_i site close to heme b_H as compared to heme b_L (Fig. 1A), in accordance with the more pronounced effect of delipidation on the midpoint potential of the former. Removal of neighbouring phosphatidyl-ethanolamine and phosphatidyl-choline molecules will affect local charge distribution and the electrostatic environment of the *b*-hemes, yet, it is not known to which extent this may lower the midpoint potentials. In addition, the observed differences will contribute to lower cyt *c* reductase activity but do not explain the nearly complete inactivation of the enzyme upon delipidation. The removal of lipids and especially of CL may have caused structural perturbances but not an irreversible damage as indicated by full reversibility of the spectral properties of the heme *b* cofactors. This assumption is supported by an electrochemically induced FTIR difference spectroscopy study which demonstrated that the delipidated complex is stable but has a perturbation in the spectral property typical for the protein backbone, which can be partially reversed by relipidation [37]. Finally, loss of the lipid layer on the surface of the quinone exchange cavity will very likely impair access of the substrates to the active sites and may thereby significantly contribute to enzyme inactivation. The different lipid-binding sites will therefore contribute differently to catalytic, spectral and electrochemical properties of the yeast cyt bc_1 complex. It was shown that destabilization of the CL_i-binding site by site-directed mutagenesis impairs the functionality of the cyt bc_1 complex [8]. Overall, the lipid complement is important for full functionality of the complex but single binding sites have to be targeted to dissect their individual contribution.

The CL_i-binding site of the yeast cyt bc_1 complex may also be important for the supramolecular assembly with COX. Based on BN-PAGE analysis of deletion variants of several subunits of individual respiratory complexes, the CL_i-binding site in the vicinity of the Q_i site (Fig. 1B) was suggested as the major interaction spot between the two respiratory enzymes [26]. Single, double and triple replacement variants of the lysine residues in the CL_i-binding site in a CL-synthesizing and CL-free environment were therefore investigated to study the influence of the modifications in this site on supramolecular association between cyt bc_1 complex and COX. BN-PAGE analysis revealed supramolecular assembly of the two enzymes in mitochondrial membranes for all variants in the CL-containing environment. In CL-free environment, supercomplex formation could not be observed for the wild-type and the single replacement variants in BN-PAGE. Surprisingly, supercomplex stability was found largely restored in two double replacement variants (K288L/K289L and K289L/K296L, but not in K288L/K296L) and in the triple replacement variant. It seems that a parallel loss of two positive charges in the CL-binding site – at the proposed interface between cyt bc_1 complex and COX – can neutralize the loss of two negative charges due to lack of CL, and therefore can restore the stability of the supercomplex association otherwise impeded by non-compensated charges. The coordination pattern from the X-ray structure suggests that the positive charge of only two of the three lysines in the CL-binding motif is neutralized upon binding of the dianionic phospholipid. Only under the condition of charge neutralization, CL seems to be no longer required for stabilization of supercomplexes. This would explain supercomplex stabilization in the double replacement variants K288L/K289L and K289L/K296L in the CL-free environment. This model is supported by the charge sensitivity of supercomplex formation. Interpretation of the electrophoretic analysis is further complicated by the possibility that other phospholipids like the acidic CL precursor phosphatidyl-glycerol may alternatively bind to the CL-binding site at the Q_i site of the cyt bc_1 complex.

5. Conclusion

This study provides direct evidence for the role of phospholipids on the catalytic, spectral and electrochemical properties of the yeast respiratory cyt bc_1 complex and on its interaction with COX. Data presented for the delipidated and relipidated enzyme indicate that individual lipid-binding sites contribute in different ways to the reversible inactivation of the enzyme. Polar lipid head groups may influence the environment of the *b*-heme cofactors with effect on absorption maxima, midpoint redox potential and catalytic activity. The analysis of supercomplex formation suggests that CL_i may serve as a charge neutralizer for the lysine residues near the presumed interaction domain between cyt bc_1 complex and COX thereby stabilising supercomplex formation. Overall, our study supports the idea, that enzyme-bound phospholipids play an important role in protein function.

Acknowledgements

We thank Christian Bach and Sofia Hollschwandner for excellent technical assistance. We thank Bernard Trumpower for the plasmids encoding wild-type and mutated *CYT1* and the yeast strain LLD6.

References

[1] A.G. Lee, How lipids affect the activities of integral membrane proteins, Biochim. Biophys. Acta 1666 (2004) 62–87.
[2] N.C. Robinson, J. Zborowski, L.H. Talbert, Cardiolipin-depleted bovine heart cytochrome *c* oxidase: binding stoichiometry and affinity for cardiolipin derivatives, Biochemistry 29 (1990) 8962–8969.
[3] P. Marius, M. Zagnoni, M.E. Sandison, J.M. East, H. Morgan, A.G. Lee, Binding of anionic lipids to at least three nonannular sites on the potassium channel KcsA is required for channel opening, Biophys. J. 94 (2008) 1689–1698.
[4] J.E. Baenziger, S.E. Ryan, M.M. Goodreid, N.Q. Vuong, R.M. Sturgeon, C.J. daCosta, Lipid composition alters drug action at the nicotinic acetylcholine receptor, Mol. Pharmacol. 73 (2008) 880–890.
[5] C. Hunte, S. Richers, Lipids and membrane protein structures, Curr. Opin. Struct. Biol. 18 (2008) 406–411.
[6] C. Hunte, Specific protein–lipid interactions in membrane proteins, Biochem. Soc. Trans. 33 (2005) 938–942.
[7] H. Palsdottir, C. Hunte, Lipids in membrane protein structures, Biochim. Biophys. Acta 1666 (2004) 2–18.
[8] C. Lange, J.H. Nett, B.L. Trumpower, C. Hunte, Specific roles of protein–phospholipid interactions in the yeast cytochrome bc_1 complex structure, EMBO J. 20 (2001) 6591–6600.
[9] M. Svensson-Ek, J. Abramson, G. Larsson, S. Tornroth, P. Brzezinski, S. Iwata, The X-ray crystal structures of wild-type and EQ(I-286) mutant cytochrome *c* oxidases from *Rhodobacter sphaeroides*, J. Mol. Biol. 321 (2002) 329–339.
[10] L. Varanasi, D. Mills, A. Murphree, J. Gray, C. Purser, R. Baker, J. Hosler, Altering conserved lipid binding sites in cytochrome *c* oxidase of *Rhodobacter sphaeroides*

perturbs the interaction between subunits I and III and promotes suicide inactivation of the enzyme, Biochemistry 45 (2006) 14896–14907.
[11] P. Mitchell, Possible molecular mechanisms of the protonmotive function of cytochrome systems, J. Theor. Biol. 62 (1976) 327–367.
[12] S. Iwata, J.W. Lee, K. Okada, J.K. Lee, M. Iwata, B. Rasmussen, T.A. Link, S. Ramaswamy, B.K. Jap, Complete structure of the 11-subunit bovine mitochondrial cytochrome bc_1 complex, Science 281 (1998) 64–71.
[13] D. Xia, C.A. Yu, H. Kim, J.Z. Xian, A.M. Kachurin, L. Zhang, L. Yu, J. Deisenhofer, Crystal structure of the cytochrome *bc*(1) complex from bovine heart mitochondria, Science 277 (1997) 60–66.
[14] Z.L. Zhang, L.S. Huang, V.M. Shulmeister, Y.I. Chi, K.K. Kim, L.W. Hung, A.R. Crofts, E.A. Berry, S.H. Kim, Electron transfer by domain movement in cytochrome bc_1, Nature 392 (1998) 677–684.
[15] C. Hunte, J. Koepke, C. Lange, T. Rossmanith, H. Michel, Structure at 2.3 angstrom resolution of the cytochrome *bc*(1) complex from the yeast *Saccharomyces cerevisiae* co-crystallized with an antibody Fv fragment, Struct. Fold. Des. 8 (2000) 669–684.
[16] C.R. Lancaster, C. Hunte, J. Kelley III, B.L. Trumpower, R. Ditchfield, A comparison of stigmatellin conformations, free and bound to the photosynthetic reaction center and the cytochrome bc_1 complex, J. Mol. Biol. 368 (2007) 197–208.
[17] H. Palsdottir, C.G. Lojero, B.L. Trumpower, C. Hunte, Structure of the yeast cytochrome bc_1 complex with a hydroxyquinone anion Qo site inhibitor bound, J. Biol. Chem. 278 (2003) 31303–31311.
[18] E.A. Berry, M. Guergova-Kuras, L.S. Huang, A.R. Crofts, Structure and function of cytochrome *bc* complexes [Review], Annu. Rev. Biochem. 69 (2000) 1005–1075.
[19] A.R. Crofts, The cytochrome bc_1 complex: function in the context of structure, Annu. Rev. Physiol. 66 (2004) 689–733.
[20] A. Osyczka, C.C. Moser, P.L. Dutton, Fixing the Q cycle, Trends Biochem. Sci. 30 (2005) 176–182.
[21] H. Schagger, T. Hagen, B. Roth, U. Brandt, T.A. Link, G. von Jagow, Phospholipid specificity of bovine heart bc_1 complex, Eur. J. Biochem. 190 (1990) 123–130.
[22] C.A. Yu, L. Yu, Structural role of phospholipids in ubiquinol–cytochrome *c* reductase. Biochemistry 19 (1980) 5715–5720.
[23] B. Gomez Jr., N.C. Robinson, Phospholipase digestion of bound cardiolipin reversibly inactivates bovine cytochrome bc_1, Biochemistry 38 (1999) 9031–9038.
[24] S.R. Solmaz, C. Hunte, Structure of complex III with bound cytochrome *c* in reduced state and definition of a minimal core interface for electron transfer, J. Biol. Chem. 283 (2008) 17542–17549.
[25] A.R. Klingen, H. Palsdottir, C. Hunte, G.M. Ullmann, Redox-linked protonation state changes in cytochrome bc_1 identified by Poisson–Boltzmann electrostatics calculations, Biochim. Biophys. Acta 1767 (2007) 204–221.
[26] K. Pfeiffer, V. Gohil, R.A. Stuart, C. Hunte, U. Brandt, M.L. Greenberg, H. Schagger, Cardiolipin stabilizes respiratory chain supercomplexes, J. Biol. Chem. 278 (2003) 52873–52880.
[27] T. Wenz, P. Hellwig, F. MacMillan, B. Meunier, C. Hunte, Probing the role of E272 in quinol oxidation of mitochondrial complex III, Biochemistry 45 (2006) 9042–9052.
[28] D. Moss, E. Nabedryk, J. Breton, W. Mantele, Redox-linked conformational changes in proteins detected by a combination of infrared spectroscopy and protein electrochemistry. Evaluation of the technique with cytochrome *c*, Eur. J. Biochem. 187 (1990) 565–572.
[29] P. Hellwig, J. Behr, C. Ostermeier, O.M. Richter, U. Pfitzner, A. Odenwald, B. Ludwig, H. Michel, W. Mantele, Involvement of glutamic acid 278 in the redox reaction of the cytochrome *c* oxidase from *Paracoccus denitrificans* investigated by FTIR spectroscopy, Biochemistry 37 (1998) 7390–7399.
[30] P. Hellwig, T. Soulimane, G. Buse, W. Mantele, Electrochemical, FTIR, and UV/VIS spectroscopic properties of the ba(3) oxidase from *Thermus thermophilus*, Biochemistry 38 (1999) 9648–9658.
[31] I. Arnold, K. Pfeiffer, W. Neupert, R.A. Stuart, H. Schagger, Yeast mitochondrial F1F0-ATP synthase exists as a dimer: identification of three dimer-specific subunits, EMBO J. 17 (1998) 7170–7178.
[32] I. Wittig, H.P. Braun, H. Schagger, Blue native PAGE, Natl. Protoc. 1 (2006) 418–428.
[33] H. Schagger, Tricine-SDS-PAGE, Natl. Protoc. 1 (2006) 16–22.
[34] H. Schagger, K. Pfeiffer, EMBO J. 19 (2000) 1777–1783.
[35] S. Drose, U. Brandt, The mechanism of mitochondrial superoxide production by the cytochrome bc_1 complex, J. Biol. Chem. 283 (2008) 21649–21654.
[36] T. Wenz, R. Covian, P. Hellwig, F. MacMillan, B. Meunier, B.L. Trumpower, C. Hunte, Mutational analysis of cytochrome *b* at the ubiquinol oxidation site of yeast complex III, J. Biol. Chem. 282 (2007) 3977–3988.
[37] R. Hielscher, T. Wenz, C. Hunte, P. Hellwig, Monitoring the redox and protonation dependent contributions of cardiolipin in electrochemically induced FTIR difference spectra of the cytochrome bc_1 complex from yeast, Biochim. Biophys. Acta 1787 (2009) 617–625.
[38] M. Yang, B.L. Trumpower, Deletion of QCR6, the gene encoding subunit six of the mitochondrial cytochrome bc_1 complex, blocks maturation of cytochrome c_1, and causes temperature-sensitive petite growth in *Saccharomyces cerevisiae*, J. Biol. Chem. 269 (1994) 1270–1275.